Effects of Bedrock Groundwater and Geological Structure on Hydrological Processes in Mountainous Watersheds

Naoya MASAOKA[1,*], Ken'ichirou KOSUGI[1,2], Masanori KATSUYAMA[3], Takahisa MIZUYAMA[1], Shusuke MIYATA[4] and Daizo TSUTSUMI[4]

[1] Graduate School of Agriculture, Kyoto University (Kitashirakawa, Sakyo-ku, Kyoto, Kyoto 6068502, Japan)

[2] CREST, JST (Sanbancho, Chiyoda-ku, Tokyo 1020075, Japan)

[3] Inter-Graduate School Unit for Sustainable Development and Survivable Societies, Kyoto University (201 Nihon Italia Kaikan, Ushinomiya-cho 4, Yoshida, Sakyo-ku, Kyoto, Kyoto 6068302, Japan)

[4] Disaster Prevention Research Institute, Kyoto University (Gokasyo, Uji, Kyoto 6110011, Japan)

*Corresponding author. E-mail: hatiemon@kais.kyoto-u.ac.jp

To survey the movement of bedrock groundwater in mountainous watersheds with heterogeneous geological structures, discharge observations were conducted together with hydrochemical analyses of major ions, SiO_2, and oxygen isotopes concentrations. Major ion concentrations clearly reflect the chemical component of local geology in each watershed, as shown in hexa-diagrams: Ca-HCO_3 type water and Ca-SO_4 type water were detected in watersheds containing granite and volcanic rock, respectively. The spatial distribution of SiO_2 concentrations and oxygen isotope ratios clearly indicate the difference of groundwater flow processes in small watersheds. Moreover, they also suggest the possibility of groundwater movement across watersheds that have a continuous distribution of geology, and no movement in watersheds with a varying geology. This suggests that the discontinuous surface of geology works as a divide for groundwater. In addition, specific discharge was high in the watershed where the groundwater movement is believed to be intercepted, suggesting that groundwater dammed by a geological boundary may result in a high discharge.

Key words: bedrock groundwater, geological structure, major ions, silica, oxygen isotope ratio

1. INTRODUCTION

Recent studies have focused on the significant effects of bedrock groundwater on hydrological processes and landslide occurrences in mountainous watersheds. However, such effects are difficult to evaluate as the movement of such water has no relationship to the surface topography. Previous studies have reported the evidence of groundwater flow across watersheds using measurement of variations in stream inflow [*Genereux et al.*, 1993] or by measuring the specific discharge of neighboring watersheds [*Inokura and Yoshimura*, 1992]. In a recent study, *Kosugi et al.* [2011] confirmed the existence of groundwater flow across a topographic boundary, by measuring the spatial distribution of groundwater table with intensive bedrock wells.

Most of these hydrological studies have been conducted in watersheds with a homogeneous geological structure. However, it is known that a heterogeneous geological structure often has a much more complicated effect on groundwater movement. Such geological boundaries often work as discontinuous surfaces of permeability, causing a local rise in the groundwater level that can result in the occurrence of landslides [e.g., *Nishiyama and Chigira*, 2001]. Fault lines sometimes show low or high permeability and work as a divide within the bedrock groundwater system [e.g., *Forster and Evans*, 1991; *Karasaki et al.*, 2012]. However, although such studies have been undertaken, only a limited number of studies have been conducted on the relationship between groundwater and geological structures in mountainous watersheds.

To clarify the role of bedrock groundwater, hydrochemical observations are effective in defining the local geology and identifying the groundwater flow path as a natural tracer. Major ion concentrations in groundwater are characterized by

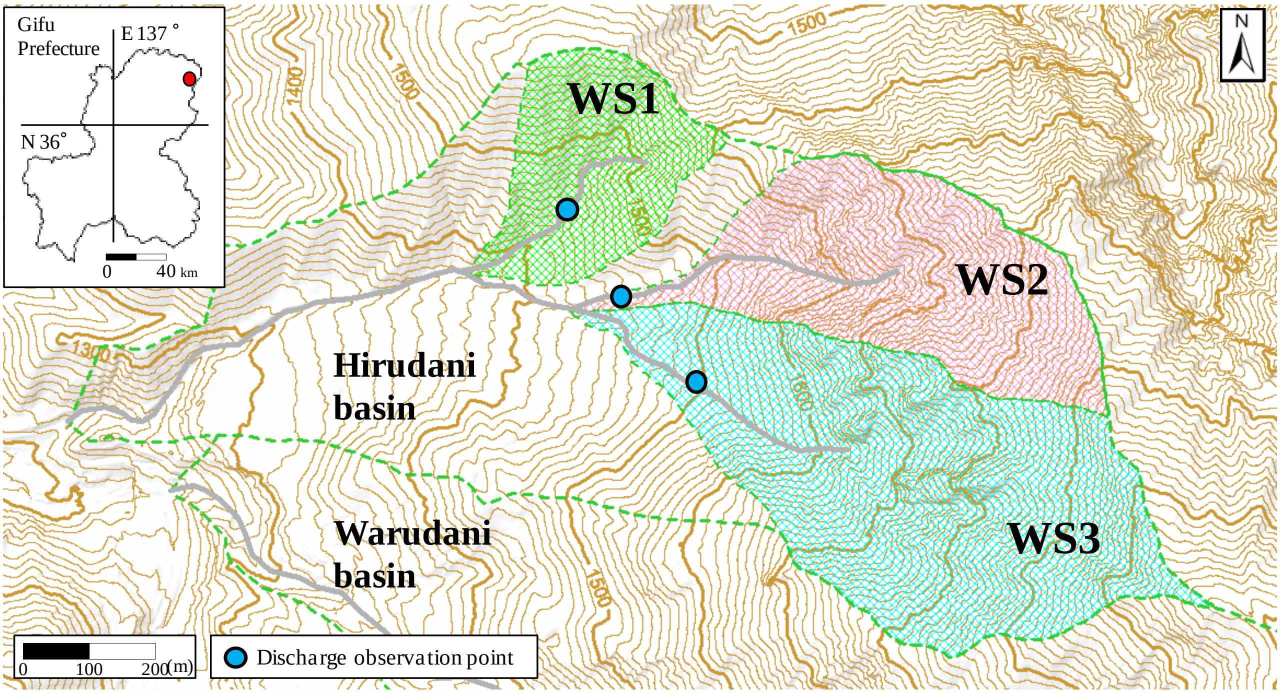

Fig. 1 Topographic map of the Hirudani experimental basin, showing the positions of small watersheds WS1, WS2, and WS3.

the chemical component and weathering degree of the rock [e.g., *Oyama et al.*, 2011]. The concentration of silica (SiO_2) is an important indicator of the water residence time in bedrock [e.g., *Burns et al.*, 2003; *Tesoriero et al.*, 2005], and is frequently used in headwater hydrological observations. In watersheds with a high specific discharge, the SiO_2 concentrations often exhibit high values, indicating a large contribution of bedrock groundwater [e.g., *Inokura and Yoshimura*, 1992; *Tsujimura et al.*, 2001; *Uchida et al.*, 2003]. Stable isotopes of water (that act as natural tracers in rainfall) provide a means of exploring the pathways of subsurface groundwater [e.g., *McGlynn et al.*, 1999]. In addition, the oxygen and hydrogen isotope ratios are highly related to rainfall altitudes [e.g., *Holdsworth et al.*, 1991], and by comparing the isotope ratios of spring water with altitudes, *Suzuki et al.* [2011] detected a spring that originated from a different groundwater flow system within a group of springs on the Hakone Caldera's outer slope.

In this study, a string of hydrochemical observations of surface water were conducted in a mountainous basin with a heterogeneous geological structure, to evaluate the effect of the geological structure on the bedrock groundwater movement and on hydrological processes within the basin.

2. SITE DISCRIPTION

Observations were performed in the Hirudani experimental basin (82.1 ha) in the Hodaka Sedimentation Observatory of the Disaster Prevention Research Institute, at Kyoto University in Gifu, central Japan (36°15'N, 137°35'E; **Fig. 1**). The mean annual air temperature is 9.5 °C, and the mean annual precipitation is 1980 mm, a quarter of which falls as snow in winter (1979 to 2013, Japan Meteorological Agency). The Warudani basin (108.2 ha) lies to the south of the Hirudani basin. The Hirudani basin contains three small watersheds, which are here referred to as WS1, WS2, and WS3 (**Fig. 1**). The area and mean gradient of each of these watersheds is summarized in **Figure 2**, together with photo images. As shown in the image, WS1 is characterized by bare slopes where sediment production during the freeze-thaw action in winter has been observed [e.g., *Fujita et al.*, 2002]. In contrast, in WS2 and WS3, there are few bare slopes, and the riparian area is covered by vegetation (as shown in the images).

The study site has a complicated geological structure. **Figure 3** shows a geological map of the Hirudani basin, and **Figure 4** summarizes the proportion of geological features in each watershed and basin. A granitic ring dike (Gp) cuts across the middle part of the Hirudani basin, covering approximately 60% of the total area of WS1, but does not exist in WS2 and WS3. Mesozoic melange (Hm) exists widely through all the watersheds and basin, and covers approximately 60% of the total area of both WS2 and WS3. Warudani lava (Lw) is

	WS 1	WS 2	WS 3
Area	8.5 ha	15.3 ha	25.8 ha
Gradient	28.2°	32.6°	32.1°
Image			

Fig. 2 Area, mean gradient, and photo images of small watersheds WS1, WS2, and WS3.

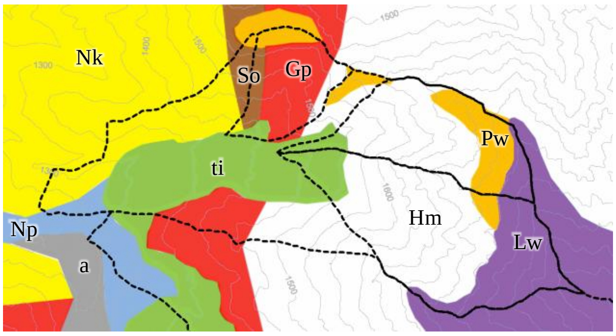

Gp: Granitic ring dike
Hm: Mesozoic melange
Lw: Warudani lava
Pw: Warudani pyroclastic rock
So: Sodegatani conglomerate member
Nk: Nakao tuff
Np: Nakao pyroclastic flow deposition
ti: Talus fan deposition, a: river deposition

Fig. 3 Geological map of the Hirudani experimental basin compiled from *Harayama* [1990].

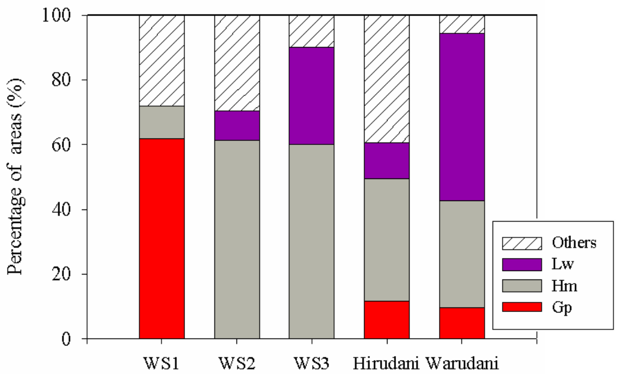

Fig. 4 Proportion of geological features in each watershed and basin.

distributed in the upstream part of the Warudani basin, where it occupies about 50% of the basin, and it then extends to WS2 and WS3 where it occupies approximately 10% and 30%, respectively.

3. METHODS

Instantaneous flow volumes were observed in the stream channels in WS1, WS2, and WS3 (**Fig. 1**) by means of the velocity-area method [*Brassington*, 2007] using electromagnetic flow meter (SF-5511, Tokyo Keisoku). The measurement was conducted on October 8, 2013, and no precipitation had been gauged in the antecedent 22 days. In WS1 and WS3, the flow volumes in stream channels were apparently small throughout the whole area even at bedrock outcrops. Because the water had high possibility to flow under the river bed at the outlet of WS1 and WS3, measurement points were selected approximately 200 m upstream of the outlet of each watershed.

Water samples were collected five times during 2010 and 2013 at 19 points within the stream and springs in and around the Hirudani basin. The concentrations of major anions (Cl^-, SO_4^{2-}) and cations (Na^+, K^+, Ca^{2+}, Mg^{2+}) were analyzed using ion chromatography (ICS-1100, Dionex). The concentration of HCO_3^- was estimated by the pH and total balance of cations and anions, the concentration of silica (SiO_2) was analyzed using ICP-AES (iCAP 6300, Thermo Scientific), and the ratio of oxygen isotope ($\delta^{18}O$) by WS-CRDS (L2120-i, Picarro). The isotope value is expressed as per mill, relative to Vienna Standard Mean Ocean Water (VSMOW).

4. RESULTS AND DISCUSSION

4.1 Discharge volume

The specific discharges in the river channels of the three watersheds showed high spatial variability. Instantaneous flow volumes observed in WS1, WS2, and WS3 (**Fig. 1**) were 0.046, 0.151, and 0.033 mm/h, respectively. Because no precipitation had been gauged in the antecedent 22 days, the measured discharge was considered to be a base

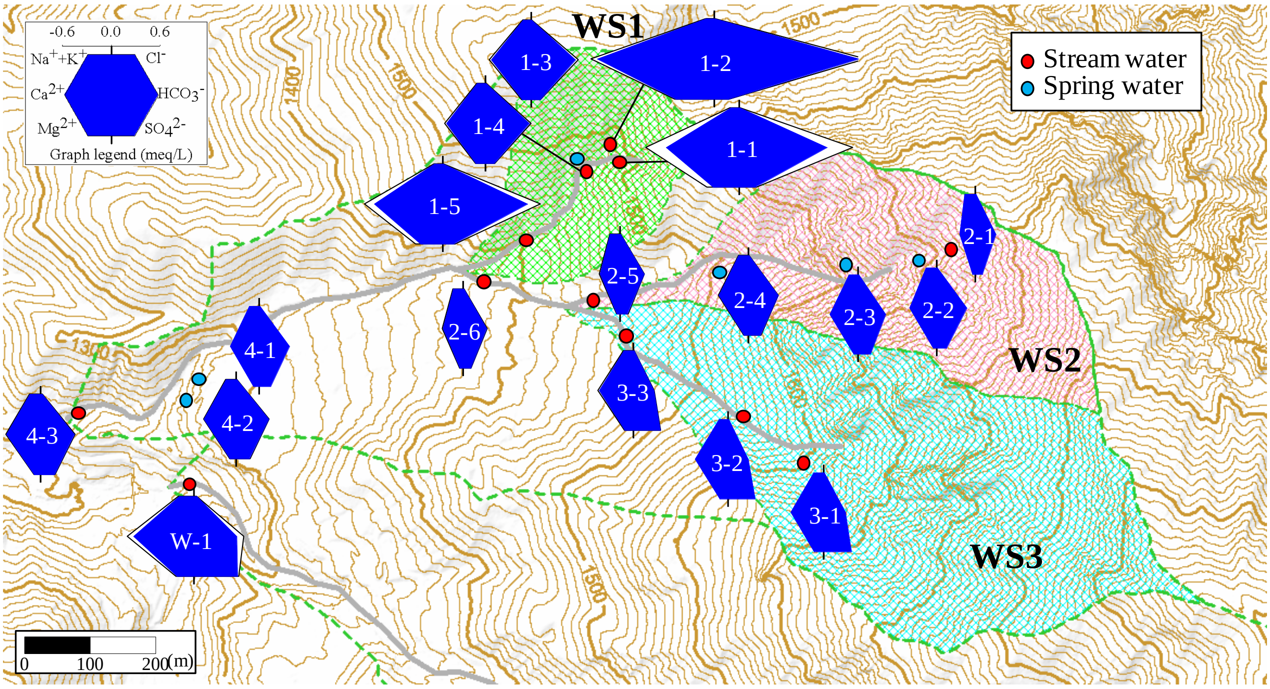

Fig. 5 Major ion concentrations, as illustrated by hexa-diagrams. Blue and white areas in diagrams indicate the average and standard error of all samples, respectively.

flow consisting mainly of bedrock groundwater seepage. Such a result suggests the existence of slower and deeper groundwater flow path at WS2, compared to these at WS1 and WS3. Moreover, it also suggests a possibility that groundwater converges on WS2 from surrounding areas crossing topographic boundaries.

4.2 Major ion concentrations

Figure 5 shows the spatial distribution of major ion concentrations, illustrated using hexa-diagrams. The hexa-diagrams in the three watersheds showed different characteristics in the type of ion concentration, but the diagrams within each watershed show similar characteristics. The ion concentration in WS1 was found to be remarkably larger than in other watersheds. In particular, there were higher concentrations of Ca^{2+} and HCO_3^- among the major ions (i.e., Ca-HCO_3 type). The ion concentration was the smallest in WS2, although the type was the same as within WS1. In WS3, however, a relatively high concentration of SO_4^{2-} was detected (i.e., Ca-SO_4 type), which was similar to the trend in the W-1 sample collected at the outlet of the Warudani basin. These trends are believed to be related to the differences in the geological structures between each small watershed, as shown in **Figure 3 and 4**. In WS1, the Ca-HCO_3 type is typically found in the shallow groundwater of the granitic area due to the dissolution of plagioclase [e.g., *Sasaki*, 2004]. In addition, in WS1 it is assumed that the ions elute faster because of the active weathering of rock on the bare slopes. Although both WS2 and WS3 are composed mainly of Hm, WS3 was found to have a higher percentage of Lw, similar to the Warudani basin (**Fig. 4**). This is in agreement with a previous report which shows that a high concentration of SO_4^{2-} tends to be found in volcanic rock [e.g., *Oyama et al.*, 2011] due to the dissolution of gypsum in volcanic ash [*Ohwada et al.*, 2007]. Thus, in this study the spatial distribution of major ion concentrations clearly reflects the local geological structure.

4.3 SiO_2 concentrations

Figure 6 shows the spatial distribution of SiO_2 concentrations (a larger circle denotes a higher concentration value). The concentrations of SiO_2 were found to be relatively high in WS2 (0.40–0.53 mmol/L), medium in WS3 (0.27–0.30 mmol/L), and low in WS1 (0.12–0.14 mmol/L). As SiO_2 concentration generally shows a strong correlation with groundwater residence time [e.g., *Burns et al.*, 2003; *Tesoriero et al.*, 2005], such a result clearly indicates that the groundwater in WS1 flows through a shallower part of the bedrock than in the other watersheds. In addition, the high SiO_2 concentration in WS2 and WS3 indicates a long and deep groundwater flow path in the bedrock, but this is not evident in WS1. This tendency is considered

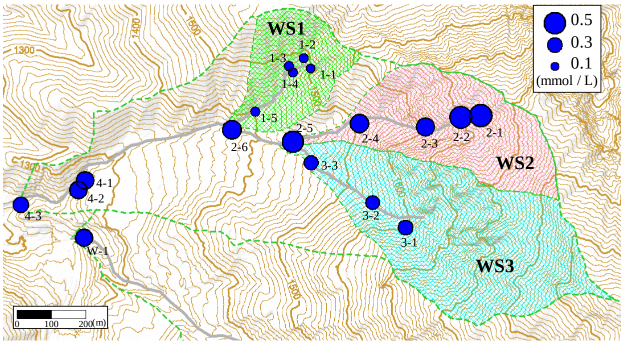

Fig. 6 Concentrations of silica (SiO_2), values are the average of all samples.

to be constant regardless of the difference in geology, because the SiO_2 concentration was low in WS1 despite the relatively high concentrations of major ions (**Fig. 5**).

It is of note that the SiO_2 concentrations exhibited quite a high value at point 2-1. From the observation of surface topography, point 2-1 and 1-3 have nearly the same catchment area. This indicates that the water at point 2-1 cannot travel on a longer and deeper flow path than at point 1-3. However, the SiO_2 concentration at point 2-1 showed quite larger value than at point 1-3. This implies therefore that the highest SiO_2 concentrations in WS2 were not only affected by deep and slow groundwater flow path, but also the groundwater traveled from higher altitudes regardless of surface topography.

4.4 Isotope ratios

Figure 7 shows the relationship between the $\delta^{18}O$ values collected on June 25, 2013 and the altitudes of the sampling points. Please note that sample a-1 was collected in the stream at a point located approximately 1 km downstream of the Hirudani basin outlet (not shown in **Fig. 1**).

The $\delta^{18}O$ values mostly decreased with the increase in altitude of the sampling points, indicating an altitude effect [e.g., *Holdsworth et al.*, 1991]. To evaluate the altitude effect of each sample clearly, a simple linear regression was fitted using the least-square method (denoted by a dotted line in **Fig. 7**). The regression line indicates "the standard altitude effect" of the study site, where a sample on the line means that water traveled a "standard distance" within the subsurface area before seeping out. If a sample is plotted on the left side of the regression line (e.g., point 2-5 in **Fig. 7**), it means that the water traveled through a relatively longer and deeper subsurface flow path. Residuals from the regression line, r, were calculated for all samples, denoted by arrows in **Figure 7**. Positive and negative values of r indicate that the water traveled along a relatively shorter and longer flow path,

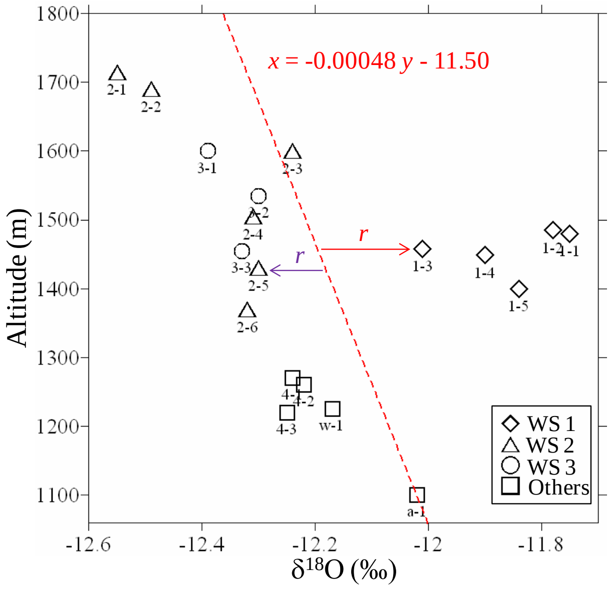

Fig. 7 Relationship between $\delta^{18}O$ values and altitudes of sampling points, red broken-line denotes simple linear regression.

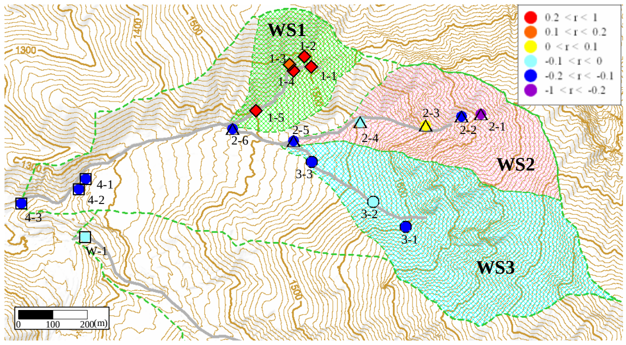

Fig. 8 Residuals from the linear regression of $\delta^{18}O$ and altitudes, r, shown in **Fig. 7**.

respectively. The spatial distribution of r is shown in **Figure 8**. Values of r for all samples in WS1 show positive values, indicating that the subsurface flow path in WS1 was relatively shorter than that of the other watersheds, where r mostly shows negative values. This result coincides with the results of SiO_2 concentrations (**Fig. 6**), which strongly suggests that the source of groundwater in WS1 is rainfall occurring in the area of WS1 only, and not accumulated groundwater from surrounding watersheds that has crossed topographic boundaries. The smallest r value for sample 2-1 (which has a small catchment area as point 1-3) also confirms the hypothesis from the results of SiO_2 concentrations (**Fig. 6**). Because r values are affected by the altitude of rainfall and not by groundwater residence time, groundwater in WS2 has a high possibility to travel from further higher altitudes by crossing topographic boundaries, not only travel through deeper and slower flow path. Thus, the spatial distribution of isotope ratios, coupled with SiO_2 concentrations, clearly demonstrates the difference of groundwater flow processes among the small watersheds. Furthermore, they strongly suggest the possibility of groundwater movement between the small watersheds.

4.5 Groundwater movement versus geological structure

It is considered that no movement of groundwater occurred between WS1 and WS2, as all hydrochemical analyses refute this supposition (**Fig. 5, 6, and 8**). Thus, the groundwater flow system in WS1 is considered to be independent of the groundwater movement in WS2 and WS3. This result agrees with the geological structure (as shown in **Fig. 3**). There is a geological boundary formed from Gp and Hm between WS1 and WS2. The difference in geology clearly correspond the difference in groundwater flow processes: the flow path in WS1 is considered to be shorter and shallower than in WS2 and WS3. Moreover, the boundary is considered to work as a discontinuous surface as it has low permeability, thus preventing groundwater movement. According to *Harayama* [1990], Gp is the ring dike intruded into the edge of the Kasagatake Caldera: the boundary between volcanic rock and the Mesozoic sedimentary rock. On the other hand, Hm belongs to the Mesozoic sedimentary rock which shows older geological age than Gp. Because Gp penetrates the geological layer vertically and deeply, the boundary of Gp and Hm has a large possibility to work as a discontinuous surface of the permeability and prevent the groundwater flow at the deeper area.

There is a possibility that this low permeable surface raises the groundwater level locally in WS2, resulting in the highest base flow discharge that was observed among the three watersheds. In contrast, continuous distributions of Lw, Pw, and Hm are shown in WS2 and WS3, where there is the possibility of groundwater movement across the watershed boundaries. Consequently, it is evident that the continuity and discontinuity of geological structures largely affect the movement of groundwater in and across watersheds.

5. CONCLUSION

Discharge observations and hydrochemical observations of major ions, SiO_2, and oxygen isotopes clarified the difference of groundwater flow processes in small watersheds. Moreover, the observations suggested the existence of bedrock groundwater movement between small watersheds across a topographic boundary. In addition, the effect of the geological structure on the bedrock groundwater movement was analyzed with the hydrological processes.

Out of the three watersheds, WS2 has the highest values of specific discharge in the river channels, implying that groundwater flow through deeper and slower flow path in WS2. Major ion concentrations clearly reflect the chemical component of the local geological structures in each watershed: $Ca\text{-}HCO_3$ and $Ca\text{-}SO_4$ type waters were detected in watersheds that contained granite (WS1) and volcanic rock (WS3), respectively. The spatial distribution of SiO_2 concentrations and oxygen isotope ratios clearly indicates the difference of groundwater flow processes in small watersheds: groundwater is considered to flow through shorter and shallower flow path in WS1, and longer and deeper in WS2 and WS3. Moreover, the water at point 2-1 (which has a small catchment area) shows the highest SiO_2 concentration and the smallest r value, suggesting the high possibility of groundwater movement across the topographic boundaries. It is therefore considered that groundwater movement occurs between neighboring watersheds that have a continuous distribution of geology (i.e., WS2 and WS3), but that no movement occurs between watersheds with different geology (i.e., the Gp and Hm boundary between WS1 and WS2). This suggests that the discontinuous surface of geology has a low permeability, and acts as a divide for the groundwater. Therefore, the groundwater dammed by the geological boundary could be the cause of the high base flow volume in WS2, where the movement of groundwater is considered to be intercepted.

This study has thus demonstrated how hydrochemical analysis can effectively investigate the bedrock groundwater flow system in mountainous watersheds with a heterogeneous geological structure. Future studies could involve conducting discharge observations and geomorphic analyses, coupled with hydrochemical observations, to establish an efficient technique for evaluating the risk of landslide occurrence using water chemistry.

ACKNOWLEDGMENT: We wish to thank K. Sugimoto, R. Nagano, and K. Takaki for their support in field measurements. This work partly supported by the River Fund in charge of River Foundation, and the Fund of Monbukagakusho for Scientific Research (22248018, 23221009).

REFERENCES

Brassington, R. (2007): *Field Hydrogeology*, John Wiley & Sons, Ltd., Chichester, U. K., pp. 106-111.

Burns, D.A., Plummer, L.N., McDonnell, J.J., Busenberg, E., Casile, G.C., Kendall, C., Hooper, R.P., Frrer, J.E., Peters, N.E., and Beven, K. (2003): The geochemical evolution of riparian ground water in a forested piedmont catchment, Ground Water, Vol. 41, pp. 913-925.

Forster, C.B. and Evans, J.P. (1991): Hydrogeology of thrust faults and crystalline thrust sheets: Results of combined field and modeling studies, Geophysical Research Letters, Vol. 18, pp. 979-982.

Fujita, M., Sawada, T., and Mizuyama, T. (2002): Monitoring of sediment movement in a small mountain watershed, INTERPRAEVENT 2002, Vol. 1, pp. 33-40.

Genereux, D.P., Hemond, H.F., and Mulholland, P.J. (1993): Spatial and temporal variability in streamflow generation on the West Fork of Walker Branch Watershed, J. Hydrol., Vol. 142, pp. 137-166.

Harayama, S. (1990): Geology of the Kamikouchi district, Geological Survey of Japan, scale 1:50,000, pp. 175 (in Japanese with English abstract).

Holdsworth, G., Fogarasi, S., and Krouse, H.R. (1991): Variation of the stable isotopes of water with altitude in the Saint Elias Mountains of Canada, J. Geophys. Res. Atmos., Vol. 96, pp. 7483-7494.

Inokura, Y. and Yoshimura, K. (1992): Runoff and water quality characteristics of small streams in mountainous drainage basins in a water shortage period, Bull. Kyushu Univ. For., Vol. 66, pp. 31-44 (in Japanese with English abstract).

Karasaki, K., Doughty, C., and Goto, J. (2012): Development of geohydrologic model of the Wildcat fault zone, TOUGH Symposium 2012, Vol. 1, pp. 1-8.

Kosugi, K., Fujimoto, M., Katsura, S., Kato, H., Sando, Y., and Mizuyama, T. (2011): Localized bedrock aquifer distribution explains discharge from a headwater catchment, Water Resour. Res., Vol. 47, W07530, doi:10.1029/2010WR009884.

McGlynn, B.L., McDonnell, J.J., Shanley, J.B., and Kendall, C. (1999): Riparian zone flowpath dynamics during snowmelt in a small headwater catchment, J. Hydrol., Vol. 222, pp. 75-92.

Nishiyama, K. and Chigira, M. (2001): Geological features of slope failures due to 1982 heavy rainfall disaster in Nagasaki, Japan, Annuals of Disas. Prev. Res. Inst., Kyoto Univ., Vol. 45, pp. 47-59 (in Japanese with English abstract).

Ohwada, M., Satake, H., Nagao, K., and Kazahaya, K. (2007): Formation processes of thermal waters in Green Tuff: A geochemical study in the Hokuriku district, central Japan, J. Volcanol. Geotherm. Res., Vol. 168, pp. 55-67.

Oyama. Y., Takahashi, M., Tsukamoto, H., Kazahaya, K., Yasuhara, M., Takahashi, H, Morikawa, N., Ohwada, M., Shibahara, A., and Inamura, A. (2011): Relationship between water quality of deep-groundwater and geology in non-volcanic areas in Japan, J. Nuclear Fuel Cycle and Environment, Vol. 18, pp. 25-34 (in Japanese with English abstract).

Sasaki, M. (2004): Geochemical features of groundwaters in granitoids, Bull. Geol. Surv. Japan, vol. 55, pp. 439-446 (in Japanese with English abstract).

Suzuki, H., Miyashita, Y., Takahashi, H., and Yasuhara, M. (2011): Chemical and isotopic compositions of spring waters on the Hakone Caldera's outer slope, Bull. Hot Spring Res. Inst., Vol. 43, pp. 29-38 (in Japanese with English abstract).

Tesoriero, A.J., Spruill, T.B., Mew, H.E., Farrell, K.M., and Harden, S.L. (2005): Nitrogen transport and transformations in a coastal plain watershed: Influence of geomorphology on flow paths and residence times, Water Resour. Res., Vol. 41, W02008, doi:10.1029/2003WR002953.

Tsujimura, M., Onda, Y., and Ito, J. (2001): Stream water chemistry in a steep headwater basin with high relief, Hydrol. Process., Vol. 15, pp. 1847-1858.

Uchida, T., Asano, Y., Ohte, N., and Mizuyama, T. (2003): Seepage area and rate of bedrock groundwater discharge at a granitic unchanneled hillslope, Water Resour. Res., Vol. 39, 1018, doi:10.1029/2002WR001298.